© 2018. Published by The Company of Biologists Ltd | Journal of Cell Science (2018) 131, jcs217406. doi:10.1242/jcs.217406

RESEARCH ARTICLE

Histone arginine methylation by Prmt5 is required for lung branching morphogenesis through repression of BMP signaling

Qiuling Li[1,*,‡], Jie Jiao[1,2,*], Huijun Li[1,2], Huajing Wan[3], Caihong Zheng[4], Jun Cai[4] and Shilai Bao[1,2,‡]

ABSTRACT

Branching morphogenesis is essential for the successful development of a functional lung to accomplish its gas exchange function. Although many studies have highlighted requirements for the bone morphogenetic protein (BMP) signaling pathway during branching morphogenesis, little is known about how BMP signaling is regulated. Here, we report that the protein arginine methyltransferase 5 (Prmt5) and symmetric dimethylation at histone H4 arginine 3 (H4R3sme2) directly associate with chromatin of *Bmp4* to suppress its transcription. Inactivation of *Prmt5* in the lung epithelium results in halted branching morphogenesis, altered epithelial cell differentiation and neonatal lethality. These defects are accompanied by increased apoptosis and reduced proliferation of lung epithelium, as a consequence of elevated canonical BMP-Smad1/5/9 signaling. Inhibition of BMP signaling by Noggin rescues the lung branching defects of *Prmt5* mutant *in vitro*. Taken together, our results identify a novel mechanism through which Prmt5-mediated histone arginine methylation represses canonical BMP signaling to regulate lung branching morphogenesis.

KEY WORDS: Arginine methylation, BMP signaling, Branching morphogenesis, Prmt5, Smad1, Smad5, Smad9

INTRODUCTION

Mammalian lung development consists of a series of remarkably elaborate branching events that drive the progression from simple lung buds to a stereotyped branching architecture to accomplish the vital function of gas exchange. In the mouse, the lung primordium arises from the ventral foregut around embryonic day (E)9.5 (Minoo et al., 1999; Wells and Melton, 1999). Once the primary lung buds have formed, they extend into the surrounding mesenchyme and begin the process of branching morphogenesis. Between E9.5 and E16.5, the primary buds generate a complex tree-like structure ending in thousands of terminal tubules through approximately 5000 times of stereotyped branching (Herriges and Morrisey, 2014; Metzger et al., 2008). The formation of a tree-like respiratory airway system is accompanied by the differentiation of epithelial cell types along the proximal-distal (P-D) axis (Domyan and Sun, 2011). The SRY-box-containing gene 2 (Sox2)-expressing proximal epithelial cells give rise to major conductive airways that are lined with ciliated, basal, neuroendocrine and secretory cells (Gontan et al., 2008; Morrisey and Hogan, 2010), whereas the Sox9/Id2-expressed distal region gives rise to the smaller bronchioles and gas exchange units that are lined with type I and type II alveolar epithelial cells (Jen et al., 1996; Liu and Hogan, 2002; Morrisey and Hogan, 2010; Rawlins, 2008).

Significant efforts have been made to identify the cellular and molecular mechanism controlling branching morphogenesis. Signaling factors, including Bmp4, Shh, Fgf10 and Wnt, play a key role in this process (Herriges et al., 2012; Herriges and Morrisey, 2014; Rock and Hogan, 2011). During branching, Fgf10 is dynamically expressed in mesenchymal clustered cells, inducing new bud formation and activation of Bmp4 and Shh pathways in the adjacent epithelium, which are responsible for the directional outgrowth of lung buds (Bellusci et al., 1997b; Lebeche et al., 1999). Both Bmp4 and Shh negatively inhibit Fgf10 activity to form a cleft, leading to bifurcation and two new bud points to finish a branching cycle (Bellusci et al., 1997a; Hyatt et al., 2002; Weaver et al., 2000). Inactivation of either Fgf10 or Shh signaling leads to complete abrogation of branching morphogenesis (Min et al., 1998; Pepicelli et al., 1998; Sekine et al., 1999), whereas inactivation of Bmp4 results in defects in branching morphogenesis and P-D airway patterning of the lung (Bellusci et al., 1996; Weaver et al., 1999). In contrast to the well-established roles of signaling factors during branching morphogenesis, relatively little is known about how these factors are regulated at transcriptional levels.

Protein arginine methyltransferase 5 (Prmt5) is a chromatin-modifying enzyme capable of catalyzing the symmetrical dimethylation of arginine residues on histone and non-histone substrates, and it plays a pivotal role in the regulation of diverse cellular processes ranging from transcription and RNA processing to signaling transduction, cell differentiation, apoptosis and organelle biosynthesis (Biggar and Li, 2015; Li et al., 2016; Stopa et al., 2015; Wang et al., 2007; Yue et al., 2013; Zhang et al., 2011; Zhou et al., 2010). Prmt5 is generally associated with transcriptional repression through methylation of histones H2A/H4R3 and H3R8 (Ancelin et al., 2006; Di Lorenzo and Bedford, 2011; Lee and Bedford, 2002; Tae et al., 2011; Tee et al., 2010; Zhang et al., 2015). In mice, Prmt5 is essential for maintaining the pluripotency of embryonic stem cells. Deletion of *Prmt5* results in the downregulation of pluripotency transcription factors and causes embryonic lethality before implantation (Tee et al., 2010). Specifically deletion of *Prmt5* in neural stem/progenitor cells leads to postnatal death in mice through reduced methylation of Sm proteins (Bezzi et al., 2013). Prmt5 is also expressed in primordial germ cell-like cells (PGCs) and directs histone arginine methylation in mouse germ cells. Inactivation of *Prmt5* in PGCs results in germ

[1]State Key Laboratory of Molecular Developmental Biology, Institute of Genetics and Developmental Biology, Chinese Academy of Sciences, Beijing 100101, People's Republic of China. [2]School of Life Sciences, University of Chinese Academy of Sciences, Beijing 100049, People's Republic of China. [3]Key Laboratory of Obstetric, Gynecologic and Pediatric Diseases and Birth Defects of the Ministry of Education, West China Institute of Women and Children's Health, and Department of Pediatrics, Huaxi Second University Hospital, Sichuan University, Chengdu, Sichuan 610041, People's Republic of China. [4]Key Laboratory of Genomic and Precision Medicine, Beijing Institute of Genomics, Chinese Academy of Sciences, Beijing 100101, People's Republic of China.
*These authors contributed equally to this work

‡Authors for correspondence (qlli@genetics.ac.cn; slbao@genetics.ac.cn)

Q.L., 0000-0002-2372-3864; H.W., 0000-0002-6041-8877

Received 2 March 2018; Accepted 19 June 2018

Journal of Cell Science (2018) 131, jcs217406. doi:10.1242/jcs.217406

cell loss during spermatogenesis (Wang et al., 2015a,b). Whether Prmt5 plays a role in lung development remains unclear.

In the present study, we found that Prmt5 is highly expressed in the lung during active branching morphogenesis. Conditional inactivation of *Prmt5* in lung epithelium results in halted branching morphogenesis and altered cell differentiation. The branching morphogenesis defects are associated with massive apoptosis and inhibited proliferation of lung epithelial cells, as a consequence of elevated and spatially disorganized expression of *Bmp4*, which is a direct target of Prmt5. These data demonstrate that lung branching morphogenesis is regulated by Prmt5 through transcriptional repression of BMP signaling, providing an intrinsic mechanism for histone methylation during embryonic lung development.

RESULTS

Inactivation of *Prmt5* in lung epithelium leads to defective lung morphogenesis and neonatal lethality

To address whether Prmt5 plays a role in lung development, we examined its spatial and temporal expression patterns by immunostaining of embryonic lung sections. We found that Prmt5 was expressed broadly throughout the lung epithelium and mesenchyme from E12.5 to E18.5, with both nuclear and cytoplasmic localization (Fig. 1A). Interestingly, Prmt5 expression was notably decreased from E14.5 to E16.5 (Fig. 1A); this decrease was further verified at the transcript level by qRT-PCR (Fig. 1B). These data imply that Prmt5 is required during embryonic lung development.

To further assess the role of *Prmt5* during embryonic lung development, we conditionally inactivated *Prmt5* in lung epithelium using a previously reported sonic hedgehog Cre line (Harfe et al., 2004; Harris et al., 2006). We bred the *Prmt5*$^{fl/fl}$ allele with *Shh*^{cre} to generate *Prmt5*$^{fl/fl}$;*Shh*$^{cre/+}$ mice (herein referred to as *Shh;Prmt5*). Specifically Cre expression in lung epithelium was detected in an mTmG reporter mouse line at E12.5 (Fig. S1A); the efficiency of Cre-mediated epithelial *Prmt5* deletion was examined by qRT-PCR, western blotting and immunostaining (Fig. 1C; Fig. S1B-E). Prmt5 expression and its catalyzed substrate H4R3sme2 were specifically absent in lung epithelium at E12.5, and their mesenchyme expression and H4R3me2 expression were not affected (Fig. 1C; Fig. S1D,E). Collectively, these experiments suggest that *Prmt5* is specifically inactivated in lung epithelium.

Shh;Prmt5 mutants survived during embryogenesis but all died at birth from respiratory distress with a cyanotic phenotype (Fig. 1D; Table S1). Examination of lungs from E18.5 *Shh;Prmt5* embryos revealed a disorganized architecture with the presence of multiple large cysts instead of well-formed lung lobes (Fig. 1E). A significant decrease in lung-to-body weight ratios was also observed (Fig. 1F; Fig. S2A), and an approximately threefold reduction in epithelial cells was consistently observed by FACS analysis in the *Shh;Prmt5* mice (Fig. S1B). Lung cysts were easily seen by E14.5 in whole mounts of lungs isolated from *Shh;Prmt5* mice, and these cysts became more apparent by E16.5 (Fig. S2B). However, an appropriate number of lung lobes was still formed in the *Shh;Prmt5* mice (Fig. S2B). Hematoxylin and eosin (H&E)-stained lung sections revealed that these cyst-like structures formed as early as E12.5 and expanded in later development, resulting in several larger and rounder open spaces in *Shh;Prmt5* lungs (Fig. S2C). These experiments suggest that the epithelial *Prmt5* is essential for embryonic lung development to form a functional lung.

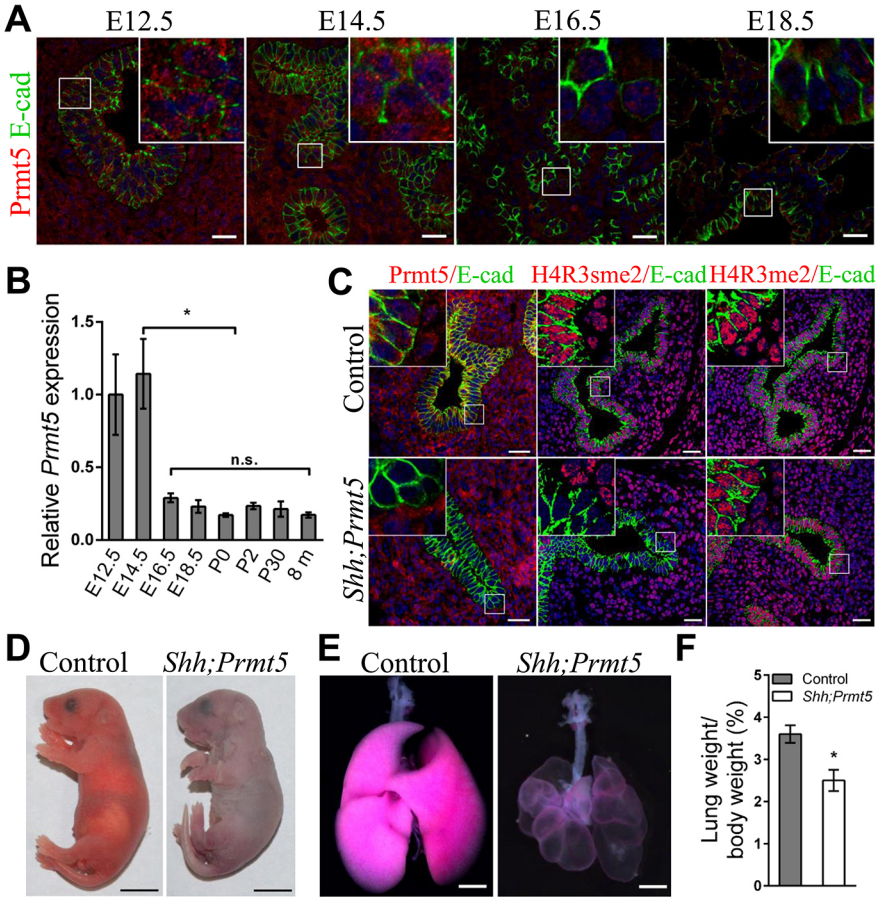

Fig. 1. Inactivation of *Prmt5* in the lung epithelium leads to lung defects and lethality at birth. (A) Representative immunostaining images showing the endogenous Prmt5 expression during lung embryonic development. Boxed regions are magnified in insets. Scale bars: 50 µm. (B) Quantification of *Prmt5* mRNA levels by qRT-PCR at the indicated developmental stages. Data were normalized to β-actin and then to the expression level at E12.5. *n*=5 biological replicates from three independent experiments. Data are represented as mean±s.e.m. **P*<0.05; n.s., not significant (one-way ANOVA followed by Tukey's test). (C) Immunostaining experiments demonstrate the loss of Prmt5 and H4R3sme2 expression in the respiratory epithelium of E12.5 *Shh;Prmt5* embryos. Boxed regions are magnified in insets. Scale bars: 50 µm. (D) Intact pups of control and *Shh;Prmt5* mutant at birth are shown. Scale bars: 0.5 cm. (E) Ventral view of dissected lungs from E18.5 control and *Shh;Prmt5* mutant. Scale bars: 1 mm. (F) Quantification of lung-to-body weight ratios of E18.5 control and *Shh;Prmt5* mutant. *n*=9 per genotype used for quantification. Data are represented as mean±s.e.m. **P*<0.05 (Student's *t*-test). E-cad, E-cadherin.

Journal of Cell Science (2018) 131, jcs217406. doi:10.1242/jcs.217406

Inactivation of *Prmt5* results in striking defects in branching morphogenesis

To evaluate whether Prmt5 regulates lung branching, we dissected lungs from control and *Shh;Prmt5* mice and performed whole-mount E-cadherin immunostaining. Lungs from *Shh;Prmt5* mice were not distinct from control at E11.5 (Fig. 2A). However, from E12.5 onwards, whereas stereotyped branching was actively underway in the control lungs, the *Shh;Prmt5* lungs stopped new branch generation, and unbranched lung buds enlarged during development and resulted in a multi-cyst structure (Fig. 2A). Consistently, we observed significantly decreased branches with cystic structures in *Shh;Prmt5* mice at E12.5 (Fig. 2B,C). We then examined the branching process by *in vitro* lung explant culture. Branching morphogenesis was halted, and no new branches were generated in *Shh;Prmt5* lungs, whereas branching occurred normally in control mice (Fig. 2B,C). Therefore, these results demonstrate that the epithelial *Prmt5* is essential for lung branching morphogenesis.

We also used an inducible gene knockout approach (Sauer, 1998; Tichelaar et al., 2000) to selectively abrogate *Prmt5* activity at different lung developmental stages. *Prmt5*$^{fl/fl}$*;SPC-rtTA;TetO-Cre* (herein referred to as *SPC;Prmt5*) triple-transgenic mice were generated by maintaining pregnant dams on doxycycline from E6.5 onwards. Immunohistochemical analysis showed specifically Cre expression and Prmt5 deletion in the epithelium of E14.5 *SPC;Prmt5* lungs (Fig. S3A). Most *SPC;Prmt5* mice died of respiratory distress shortly after birth. However, some *SPC;Prmt5* mice (13 of 83 from 10 litters, *SPC;Prmt5* mice with doxycycline vs. 21 of 81 from 9 litters, *SPC;Prmt5* mice without doxycycline) survived to adulthood with multiple large cysts at the distal epithelial branch (Fig. S3B). Histologic analysis showed that the *SPC;Prmt5* mice exhibited cyst-like structures in the distal regions of the lung at E14.5 and E18.5 (Fig. S3C), similar to what has been observed in *Shh;Prmt5* mice. Interestingly, enlarged airspaces were observed in mature lungs of *SPC;Prmt5* mice that were maintained on doxycycline from E12.5 onwards, whereas no morphologic abnormalities were observed in the lungs of *SPC;Prmt5* mice that were maintained on doxycycline from E14.5 onwards (Fig. S3C). Quantitative analysis of *in vitro* cultured lungs showed a significant reduction in branching in *SPC;Prmt5* mice compared with controls, whereas no significant differences were observed at the start of culture, E12.5 (Fig. S3D,E). Collectively, these data further demonstrate that epithelial *Prmt5* is necessary for lung branching morphogenesis.

Prmt5 is required for proximal epithelial cell differentiation in the developing lung

To assess further the molecular effects of *Prmt5* inactivation on lung branching morphogenesis, we performed whole-mount immunofluorescence co-staining to examine the expression of a distal marker Sox9 and a proximal marker Sox2 (Gontan et al., 2008; Perl et al., 2005; Que et al., 2007). In *Shh;Prmt5* mice at E11.5, Sox2 and Sox9 expressions were comparable to controls (Fig. 3A). However, although the Sox2^{+} region aggressively extended accompanied by branching morphogenesis in later developmental stages, it remained largely unchanged in *Shh;Prmt5* lungs (Fig. 3A,B). Conversely, although Sox9 was expressed in the distal epithelium in the control lung, it was expanded to most of the lung epithelium in the *Shh;Prmt5* mice (Fig. 3A,B). Consistently, clearly reduced Sox2 and expanded Sox9 expression areas were detected in the E14.5 *Shh;Prmt5* lung sections (Fig. 3C). These changes were further supported by qRT-PCR results from FACS-purified lung epithelium showing decreased *Sox2* and increased *Sox9* mRNA expressions in *Shh;Prmt5* mutant lungs compared with controls (Fig. 3D). Collectively, these observations reveal that the dilated branch tips express Sox9 and the few branch stalks express Sox2 in *Shh;Prmt5* lungs.

Next, we investigated whether loss of *Prmt5* affects epithelial cell differentiation. All analyzed early-airway epithelial markers, including Sox2, Sox9, Nkx2.1, Sftpc, SSEA1 and E-cadherin,

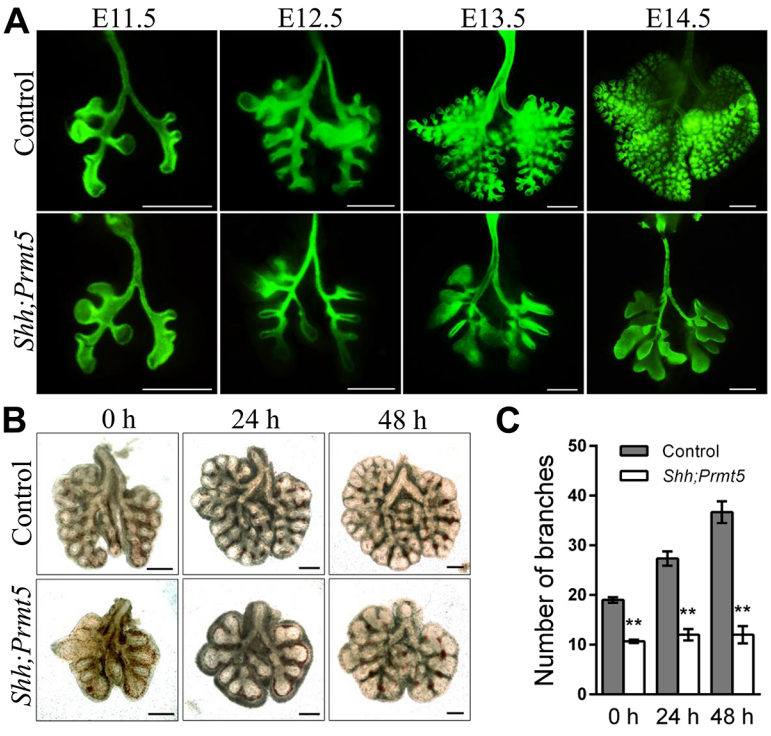

Fig. 2. Inactivation of *Prmt5* results in defects in lung branching morphogenesis. (A) Representative controls and *Shh;Prmt5* lungs from E11.5 to E14.5 with the epithelium outlined by whole-mount E-cadherin immunostaining. Scale bars: 500 µm. (B) Whole-mount images of E12.5 controls and *Shh;Prmt5* explant lungs cultured immediately after dissection (0 h) and after 24 h or 48 h in culture. Scale bars: 200 µm. (C) Quantification of the number of branches for panel B. *n*=9 biological replicates from three independent experiments. Data are represented as mean±s.e.m. ***P*<0.01 (Student's *t*-test).

Journal of Cell Science (2018) 131, jcs217406. doi:10.1242/jcs.217406

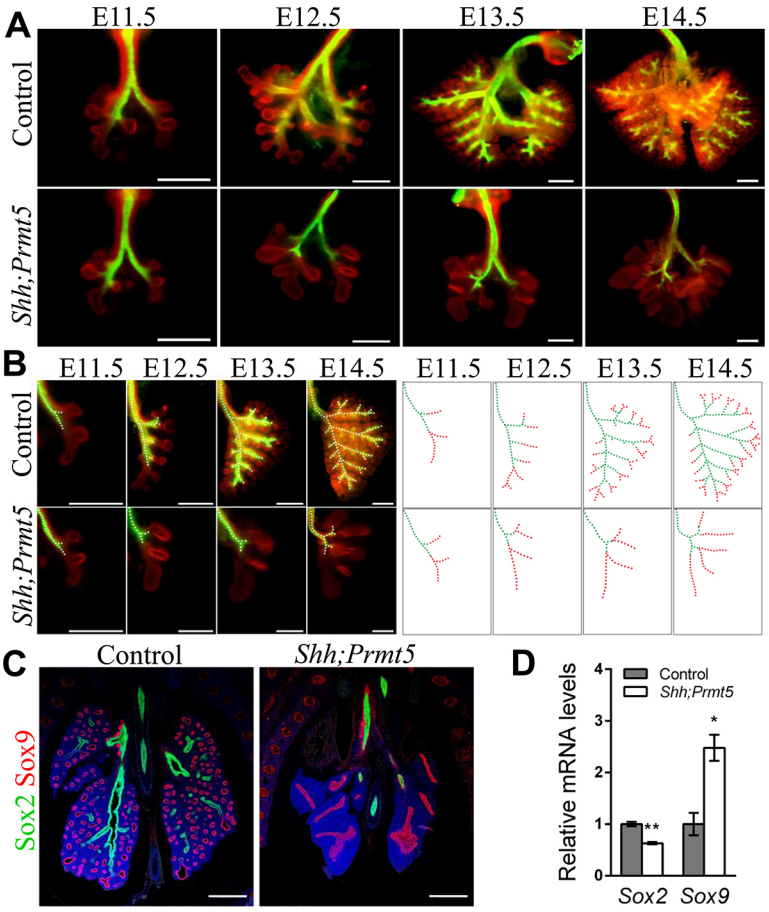

Fig. 3. Increased Sox9 and decreased Sox2 expression in the lung of *Shh;Prmt5* mice. (A) Representative control and *Shh;Prmt5* lungs co-stained with Sox2 (green) and Sox9 (red). Scale bars: 500 µm. (B) Left lobes from panel A were isolated and photographed. Sox2-positive areas are outlined with white lines (left panel); Sox2-positive areas (green lines) and Sox9-positive areas (red lines) are illustrated in the schematics (right panel). Scale bars: 500 µm. (C) Representative sectional staining showing fewer Sox2-positive cells and expanded areas of Sox9-positive cells in E14.5 *Shh;Prmt5* lungs. Scale bars: 500 µm. (D) Quantification of *Sox2* and *Sox9* expression by qRT-PCR in E14.5 FACS-isolated lung epithelium. Quantification was carried out in n=3 biological replicates from three independent experiments. Data are represented as mean±s.e.m. *P<0.05; **P<0.01 (Student's t-test).

expressed in the E12.5 *Shh;Prmt5* lungs (Fig. 4A). Expression of α-smooth muscle actin (α-SMA), a marker of airway smooth muscle differentiation, appeared to be well maintained around conducting airways in *Shh;Prmt5* lungs at E12.5 and E14.5 (Fig. 4A). The generation of distal epithelial cell types, including alveolar type II cells (Abca3$^+$, Sftpc$^+$, Sftpd$^+$) and type I (Ager$^+$, Aqp5$^+$) cells, were observed in cystic epithelium of E18.5 *Shh;Prmt5* mice (Fig. 4B). However, neither ciliated (Ac-tub$^+$) nor neuroendocrine cells

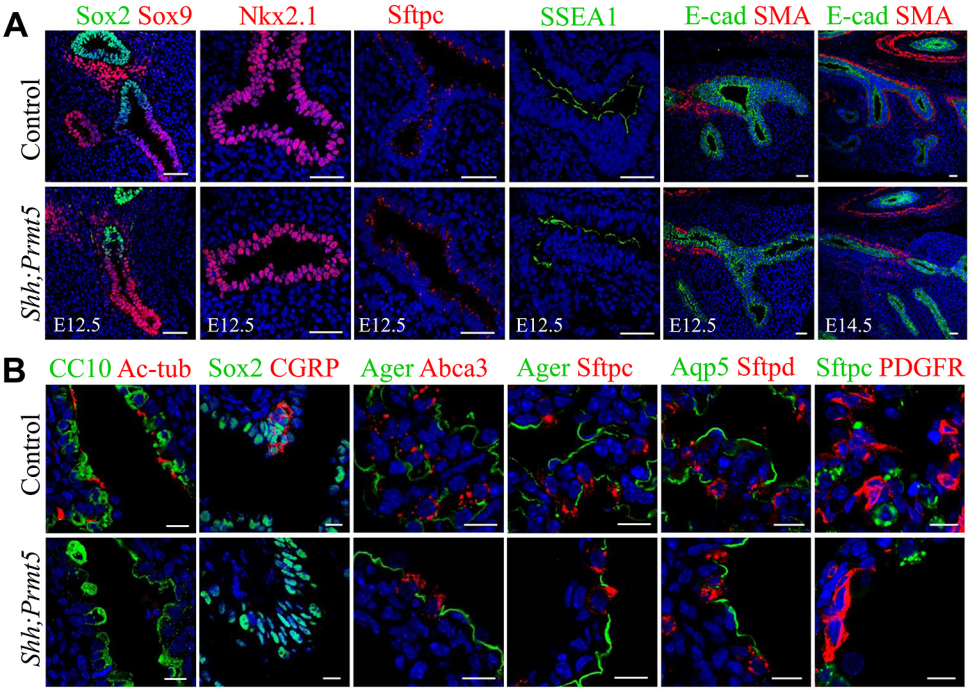

Fig. 4. Abnormal cell differentiation in lung epithelium of *Shh;Prmt5* mice. (A) Representative immunostaining images showed that lung epithelial markers, as well as the mesenchymal marker SMA, are expressed normally in *Shh;Prmt5* mice. Scale bars: 100 µm. (B) Representative immunostaining images of E18.5 lung sections by indicated antibodies. Note that the ciliated cells (Ac-tub$^+$) and neuroendocrine cells (CGRP$^+$) are undetectable in *Shh;Prmt5* lungs, and the expression of the secretory Clara cells (CC10$^+$) and proximal cell marker (Sox2$^+$) were unchanged. Alveolar type II (Abca3$^+$, Sftpc$^+$, and Sftpd$^+$) and type I (Ager$^+$ and Aqp5$^+$) specific distal epithelial markers and mesenchymal progenitor marker (PDGFR$^+$) are expressed in *Shh;Prmt5* lungs. Scale bars: 20 µm. E-cad, E-cadherin.

Journal of Cell Science (2018) 131, jcs217406. doi:10.1242/jcs.217406

(CGRP$^+$) were detected in the proximal airways of *Shh;Prmt5* lungs at E18.5 (Fig. 4B). These observations indicate that disorganization of the lung structure is associated with defective epithelial specification in the proximal airways of *Shh;Prmt5* mice.

Inactivation of *Prmt5* results in increased apoptosis and decreased proliferation in lung epithelium

To address the mechanism of lung defects in *Shh;Prmt5* mice, microarray and RNA-sequencing (RNA-seq) analyses were performed. We found that the expressions of some cell cycle regulators were changed in *Prmt5* mutant lungs (Fig. S4A, Table S2). *p21* (Cdkn1a), a known direct target of Prmt5 (Zhang et al., 2015), was also upregulated in *Prmt5* mutant mice (Fig. S4A, Table S2). We then determined whether cell apoptosis and proliferation were affected in *Shh;Prmt5* lungs. By TUNEL assay and cleaved caspase-3 (CC3) immunostaining, we observed significantly increased apoptosis in the epithelium of *Shh;Prmt5* lungs (Fig. 5A,C; Fig. S4B). Interestingly, this increase in apoptosis seemed to spatially restrict in particular epithelial regions. We then determined the percentage of proximal (Sox2$^+$ and CC3$^+$) and distal (Sox9$^+$ and CC3$^+$) apoptosis in the epithelium of control and *Shh;Prmt5* lungs. We found that proximal epithelial apoptosis was significantly higher than distal epithelial apoptosis in *Shh;Prmt5* lungs at both E11.5 (Fig. S4C,D, Movie 1) and E12.5 (Fig. 5B,D). We then analyzed epithelium proliferation by Ki67 immunostaining. The numbers of Ki67-positive cells were significantly decreased in total epithelium of *Shh;Prmt5* lungs (Fig. 5A,C). The reduced proliferation of lung epithelium was also demonstrated by pH3 immunostaining, a marker for cells in late G2 and mitosis (Fig. 5A,C). No significant changes were observed in proliferation between proximal and distal epithelium in *Shh;Prmt5* lung tissues (Fig. 5B,D; Fig. S4C,D), and both apoptosis and proliferation were not significantly affected in the mesenchyme of *Shh;Prmt5* lungs (Fig. 5C; Fig. S4D). Thus, Prmt5 controls epithelial apoptosis and proliferation during embryonic lung development.

Previous studies have shown that the cell cycle inhibitor *p21* is a Prmt5 substrate in regulating cell proliferation and apoptosis in several organs (Hu et al., 2015; Zhang et al., 2015), raising the possibility that *p21* regulates apoptosis and proliferation in the lung epithelium. Indeed, we detected an increased *p21* mRNA expression in *Prmt5* mutant lungs by microarray, RNA-seq and qRT-PCR analysis (Table S2, Figs S4A and S5A). We then expected that knockout *p21* in the *Shh;Prmt5* background would rescue lung developmental defects in *Shh;Prmt5* mice. However, branching defects and changes of epithelial apoptosis and proliferation were not affected by *p21* inactivation (Fig. S5B-D),

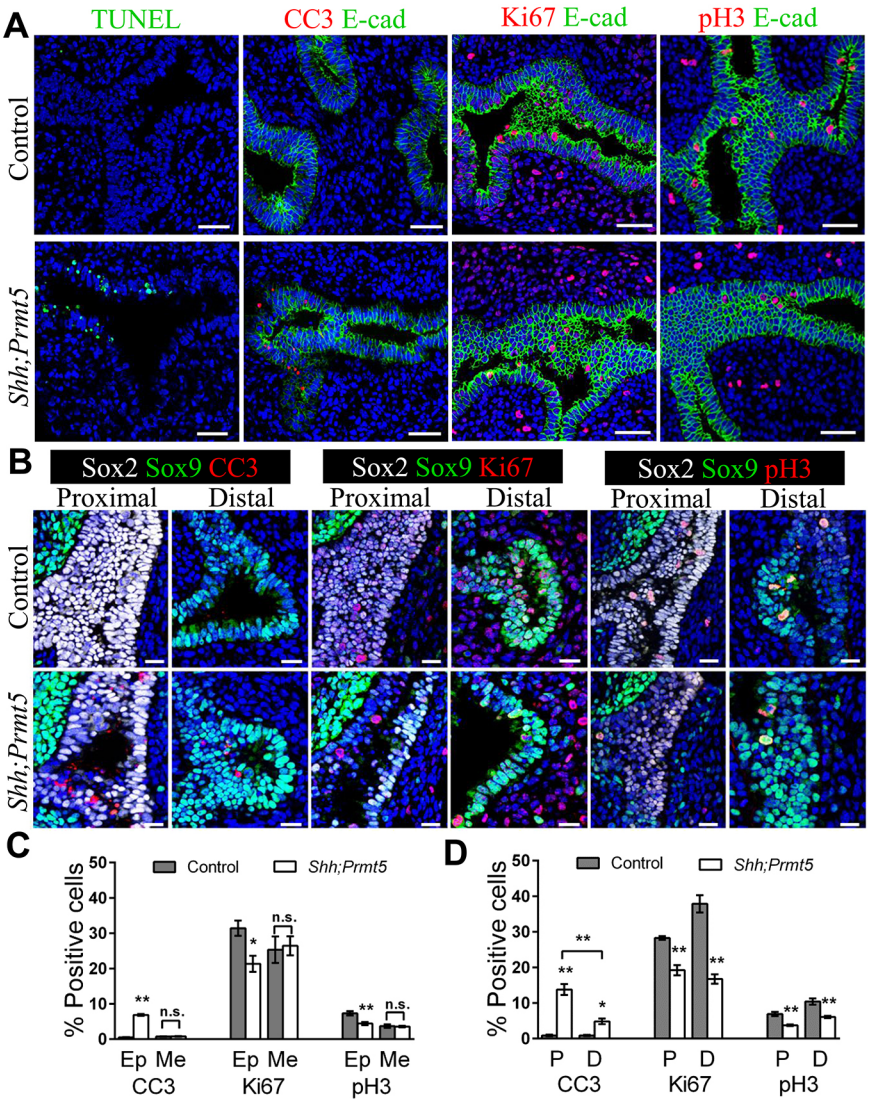

Fig. 5. Increased apoptosis and reduced proliferation in lung epithelium from *Shh;Prmt5* mice. (A) TUNEL assay and immunostaining of CC3, Ki67, and pH3 showed massive apoptosis and decreased cell proliferation in lung epithelium of E12.5 *Shh;Prmt5* mice. Scale bars: 50 µm. (B) Representative images of immunostained E12.5 lung sections by indicated antibodies. Note that apoptosis is significantly higher in proximal epithelium than in distal epithelium in E12.5 *Shh;Prmt5* lungs. Scale bars: 20 µm. (C,D) Quantitative analysis of apoptosis and proliferation in control and *Shh;Prmt5* lungs as shown in panels A (C) and B (D), respectively. Dramatically increased apoptosis and reduced proliferation are seen in the epithelium of *Shh;Prmt5* lungs, whereas no changes are seen in the mesenchyme. Quantification was carried out in n=5 samples. Data are represented as mean±s.e.m. *P<0.05; **P<0.01; n.s., not significant (one-way ANOVA with Sidak's test). E-cad, E-cadherin.

Journal of Cell Science (2018) 131, jcs217406. doi:10.1242/jcs.217406

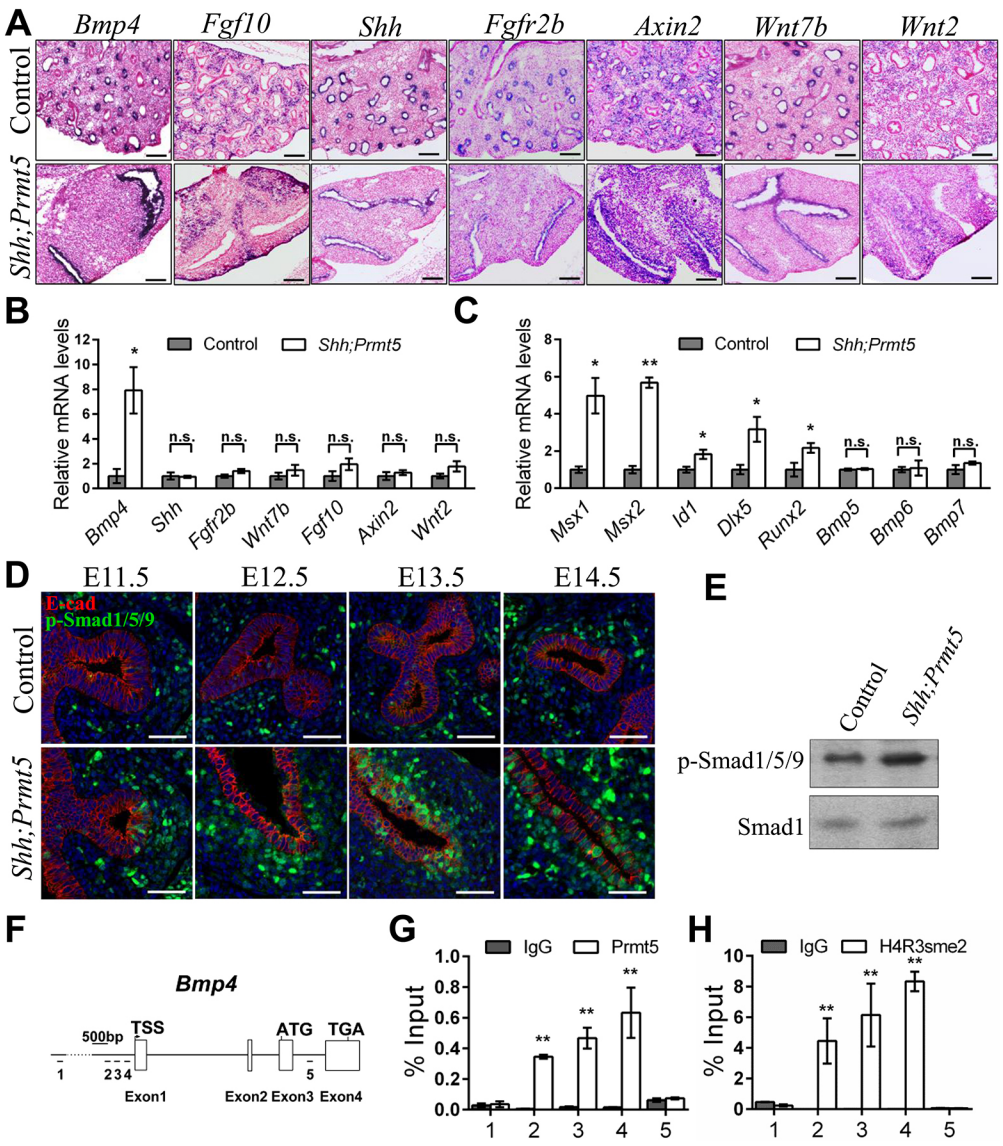

Fig. 6. Canonical BMP-Smad1/5/9 signaling is activated in *Shh;Prmt5* mice. (A) Increased and spatial-altered *Bmp4* expression in *Shh;Prmt5* lungs revealed by *in situ* hybridization. Scale bars: 200 µm. (B) qRT-PCR expression analysis revealed increased *Bmp4* expression in E14.5 FACS-isolated lung epithelium. (C) qRT-PCR validation of expression for BMP family and its downstream genes. (B,C) Quantification was carried out in n=5 biological replicates. Data are represented as mean±s.e.m. *P<0.05; **P<0.01; n.s., not significant (Student's t-test). (D) Representative immunostaining images showing the evaluated p-Smad1/5/9 expression in *Shh;Prmt5* mice through E11.5 to E14.5. Epithelial cells were outlined by anti-E-cadherin immunostaining. Scale bars: 50 µm. (E) Western blot analysis showing the increased p-Smad1/5/9 level in E14.5 *Shh;Prmt5* lungs; Smad1 was used as loading control. (F) Schematic diagrams of the *Bmp4* gene structure, with bars representing the regions examined by ChIP, as shown in panels G and H. White boxes represent exons; black lines represent introns. (G,H) ChIP assay for *Bmp4* performed with anti-Prmt5 (G) and anti-H4R3sme2 (H) antibodies, respectively. Prmt5 and H4R3sme2 directly bind to the *Bmp4* promoter at a region between 236 bp and 1136 bp upstream from the transcription start site (TSS), whereas an intergenic DNA region and a region 2-Mb upstream of *Bmp4* are not binding. All fold changes were normalized to input. Data shown are the mean±s.e.m of three independent experiments. **P<0.01 (Student's t-test).

suggesting that the function of Prmt5 in regulating cell apoptosis and proliferation during embryonic lung development is *p21*-independent.

Activated canonical BMP-Smad1/5/9 signaling in *Shh;Prmt5* mice

To assess further the molecular mechanism that underlies branching defects in *Prmt5* mutants, we examined the expression of multiple pathways known to regulate lung branching morphogenesis, including *Bmp4*, *Shh*, *Wnt* and *Fgf10* (Herriges and Morrisey, 2014). *In situ* hybridization showed that *Bmp4* expression was elevated and expanded in the epithelium of *Shh;Prmt5* lungs instead of being expressed at the distal tip of the branching airways, as observed in the control lungs (Fig. 6A) and as has been previously reported (Alanis et al., 2014; Bellusci et al., 1996; Weaver et al., 1999). Consistent with the *in situ* results, significantly increased *Bmp4* expression was also detected by qRT-PCR (Fig. 6B). In contrast, the expression of other checked genes, including *Fgf10*, *Shh*, *Wnt2*, *Wnt7b*, *Fgfr2b* and *Axin2*, were not significantly altered (Fig. 6A,B). Many BMP signaling-related genes were also differentially expressed in *Prmt5* mutant, in both microarray and RNA-seq analyses (Table S2). Several described downstream effectors of canonical BMP signaling (Holleville et al., 2003; Hollnagel et al., 1999; Shen et al., 2014) were also significantly upregulated in *Shh;Prmt5* lungs, whereas the expression of other BMP family members was not affected (Fig. 6C). Moreover, the phosphorylated Smad1/5/9, which is a direct readout of canonical BMP signaling (Moustakas and Heldin, 2009), was strongly expressed in the pulmonary epithelium and the mesenchyme surrounding the epithelium in *Shh;Prmt5* lungs from E11.5 to E14.5 (Fig. 6D). In addition, western blot analysis detected increased p-Smad1/5/9 expression (Fig. 6E). These results demonstrate that canonical BMP-Smad1/5/9 signaling is activated in *Shh;Prmt5* mice. We further determined whether *Bmp4* is a direct target of Prmt5 by chromatin immunoprecipitation (ChIP) assays, using Prmt5 and H4R3sme2 antibodies. We observed that Prmt5 and H4R3sme2 were able to bind to the promoter region of *Bmp4* at E12.5 (Fig. 6F-H). In contrast, Prmt5 and H4R3sme2 binding was not observed in an unrelated intergenic region and at 2 megabases upstream of the *Bmp4* locus (Fig. 6F-H). Together, the results of these experiments suggest that Prmt5 and H4R3sme2 directly regulate *Bmp4* transcription in the developing lung.

Journal of Cell Science (2018) 131, jcs217406. doi:10.1242/jcs.217406

Inhibition of BMP signaling rescues branching morphogenesis defects in *Shh;Prmt5* lungs

Previous reports suggested that BMP signaling plays an important role in both lung branching morphogenesis and P-D epithelium specification (Bellusci et al., 1996; Wang et al., 2013b; Weaver et al., 1999). To determine whether the activation of BMP-Smad1/5/9 signaling in the *Prmt5* mutant contributes to the lung defects described above, we inhibited BMP signaling by using the BMP antagonist Noggin (Geng et al., 2011) in an *in vitro* lung culture system. Administration of Noggin in culture was effective in reducing the expression of the canonical BMP signaling pathway readout p-Smad1/5/9, as determined by western blotting and immunostaining (Fig. S6A,B). Furthermore, *Shh;Prmt5* lungs cultured in control medium retained their dilated epithelial tip phenotype and evaluated p-Smad1/5/9 level, recapitulating the *in vivo* phenotype (Fig. 7A,B; Fig. S6B), suggesting that this *in vitro* lung culture system would allow us to examine how BMP signaling contributes to the defects in *Shh;Prmt5* lungs. Treatment of *Shh;Prmt5* lung explants with Noggin led to a significantly increased tip number, accompanied by smaller epithelial tip size, with morphology similar to that observed in control lungs (Fig. 7A,B). Furthermore, in Noggin-treated *Shh;Prmt5* lungs, the Sox2 expression domain extended farther from the point where the main bronchi split than it did in Noggin-free culture conditions, and more Sox2-expressing secondary branches were also detected (Fig. 7A,B). On the cellular level, epithelial apoptosis and proliferation were rescued significantly in *Shh;Prmt5* lung explants treated with Noggin (Fig. 7C,D). However, no ciliated cells (Ac-tub^{+}) were observed in the proximal regions of Noggin-treated *Shh;Prmt5* lungs (Fig. S6C), suggesting that other Prmt5 effectors instead of BMP signaling were involved for proximal epithelium specification. In summary, these studies suggest that the activated canonical BMP signaling significantly contributes to the lung branching morphogenesis defects in the *Shh;Prmt5* lungs.

A previous study identified Hdac1/2, an epigenetic regulator, as a repressor of Bmp4 expression through H3K9ac during embryonic lung development (Wang et al., 2013b), raising the possibility that Prmt5 and Hdac1/2 form a complex and that both H3K9ac and H4R3sme2 are required for *Bmp4* repression in *Prmt5* mutant. To address this, we first examined the expression of *Hdac1/2* and its downstream target genes by qRT-PCR. Except for *p21*, no significant differences were found between control and *Shh;Prmt5* lungs (Fig. S7A). Western blotting confirmed that Hdac1/2 and H3K9ac expressions were not affected by *Prmt5* knockout (Fig. S7B). In co-immunoprecipitation experiments, no detectable interactions between Prmt5 and Hdac1/2 were observed (Fig. S7C). Moreover, we detected a specific binding of Prmt5/H4R3sme2 with H4R3sme2 but not for H3K9ac (Fig. S7D), a histone mark that was modified by Hdac1/2 to repress *Bmp4* expression (Wang et al., 2013b). In summary, these experiments indicate that Prmt5 and Hdac1/2 function independently to repress *Bmp4* expression during lung development.

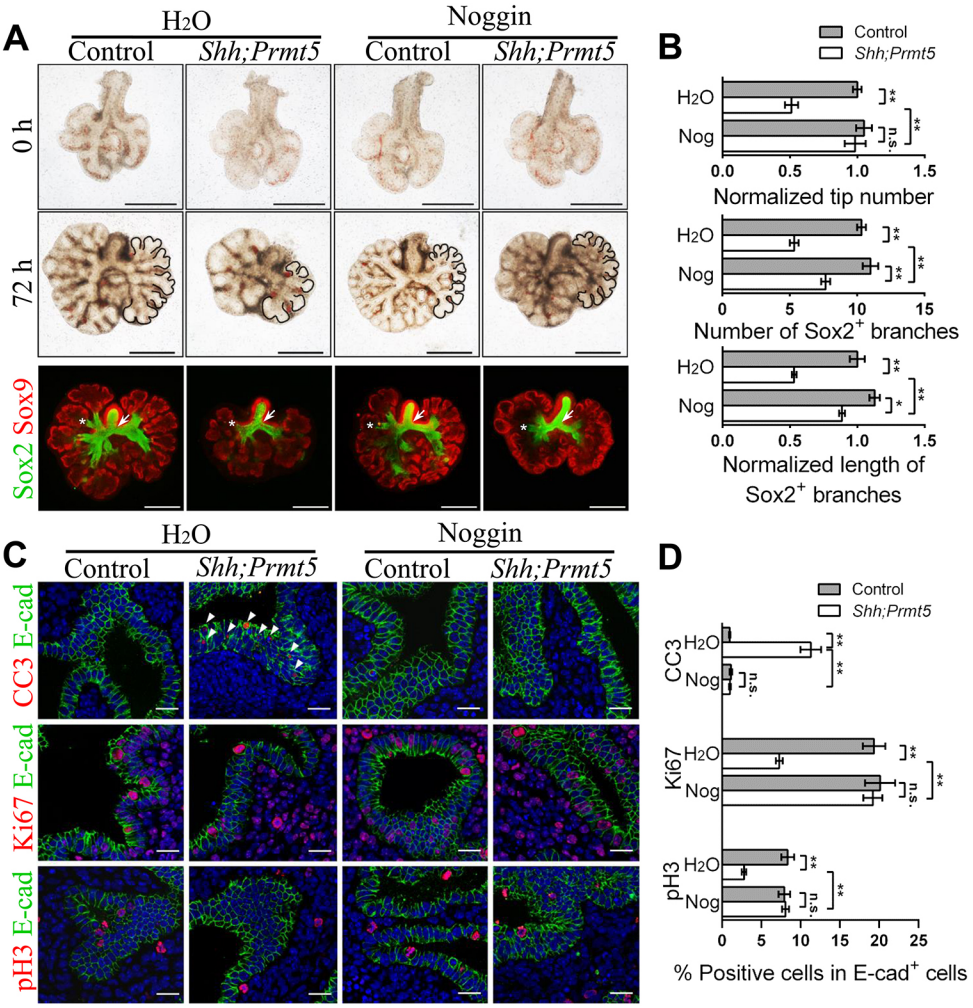

Fig. 7. Noggin treatment rescues lung developmental defects in *Shh;Prmt5* mice. (A) Representative images of lung explants showing that both tip number and Sox2^{+} stalks are rescued in *Shh;Prmt5* mice after 72 h of Noggin treatment. Tip areas of the left lobe are outlined with black lines. Arrows indicate the position where the main bronchi split. Asterisks serve as reference points indicating the distal points of Sox2 expression domain. Scale bars: 500 µm. (B) Quantification of the lung tip number, and number and length of Sox2^{+} branches, after 72 h in culture. The epithelial tips were manually counted. The lengths of Sox2^{+} branches were measured by imaging software (Nikon NIS-Elements BR V3.20). Tip numbers and length of Sox2^{+} branches in control lungs without Noggin were both set to 1. (C) Representative confocal images of sectional immunostaining for CC3, Ki67 and pH3. Note that increased apoptosis and decreased proliferation in *Shh;Prmt5* lung epithelium were significantly rescued by Noggin treatment. Scale bars: 20 µm. Arrowheads indicate CC3^{+} cells. (D) Quantification of the number of CC3^{+}, Ki67^{+}, and pH3^{+} cells in E-cadherin^{+} (E-cad^{+}) cells. (B,D) n=9 biological replicates from three independent experiments. Data are represented as mean ±s.e.m. *P<0.05; **P<0.01; n.s., not significant (one-way ANOVA with Tukey's test).

Journal of Cell Science (2018) 131, jcs217406. doi:10.1242/jcs.217406

DISCUSSION

In the present study, we provide convincing evidence that protein arginine methyltransferase Prmt5 is required for lung branching morphogenesis through repression of BMP signaling. We propose that activated canonical BMP-Smad1/5/9 signaling resulting in a halted branch cycle, accompanied by massive apoptosis and reduced proliferation in lung epithelium of *Prmt5* mutants, which eventually forms a lung with fewer and large cystic tips (Fig. 8). We identified an intriguing epigenetic mechanism whereby Prmt5-mediated H4R3sme2 transcriptionally represses *Bmp4* expression to regulate lung branching morphogenesis.

Our results indicate an important role for histone methylation in lung branching morphogenesis. First, experiments on both *Shh;Prmt5* and *SPC;Prmt5* mice demonstrated that epithelial *Prmt5* is required during lung branching morphogenesis. Second, the temporal expression pattern of Prmt5 is correlated with its crucial role in branching morphogenesis, as higher Prmt5 expression was detected before E16.5, which is when the lung buds undergo active branching to generate a tree-like network of airways (Herriges and Morrisey, 2014; Metzger et al., 2008). Finally, the critical role of Prmt5 in branching morphogenesis is further supported by the results from *SPC;Prmt5* mice, in which deletion of *Prmt5* before or after E14.5 resulted in cyst-like lung structures or no morphologic abnormalities, respectively. To our knowledge, this is the first study to show that lung branching morphogenesis is regulated by a protein methylation writer. Before our present investigation, previous studies suggested that the chromatin-remodeling factor Hdac1/2 represses *Bmp4* expression through H3K9 acetylation (Wang et al., 2013b). Of note, our experiments indicate that these two histone modifications, H4R3 dimethylation and H3K9 acetylation, function independently for *Bmp4* repression during early lung development.

We identified Bmp4 as a direct target of transcriptional repression by Prmt5 through H4R3 symmetric dimethylation (H4R3sme2). This finding is consistent with the concept that the histone mark H4R3sme2 suppresses gene transcription (Tae et al., 2011; Wang et al., 2007; Xu et al., 2010; Zhang et al., 2011). Bmp4 is an evolutionarily conserved, secreted molecule that is implicated in lung initiation (Domyan et al., 2011) and embryonic development (Hogan, 1996). Excessive BMP signaling, achieved by either overexpressing Bmp4 in lung epithelium (Bellusci et al., 1996) or knocking out the endogenous Bmp4 antagonist Gremlin (Michos et al., 2004), resulted in abnormal fetal lung formation. Our study provides mechanism evidence on how *Bmp4* is regulated at the transcriptional level. However, our discovery of elevated canonical BMP-Smad1/5/9 signaling in *Shh;Prmt5* lungs is complementary to the finding of a prior study by Norrie et al., which found an increased *Bmp4* expression by loss of *Prmt5* in limb progenitor cells (Norrie et al., 2016). The authors reported that a non-canonical Bmp4-p38 pathway, instead of a canonical BMP-Smad1/5/9 pathway, plays a dominant role (Norrie et al., 2016). We speculate that the disparity in these two mechanisms could be due to tissue- or cell-specific effects, given that Prmt5 was reported to play distinct roles in different organ contexts (Bezzi et al., 2013; Norrie et al., 2016; Wang et al., 2015b; Zhang et al., 2015). Another possible explanation is that Prmt5 has a more profound role in development through regulating canonical BMP-Smad1/5/9 signaling, as the authors stated that there might be a mild or transient increased canonical Bmp4 activity that was not detectable in their experiments (Norrie et al., 2016).

Our study indicates that BMP signaling regulates epithelial apoptosis and proliferation during embryonic lung development. Specifically, elevated BMP-Smad1/5/9 signaling results in massive apoptosis and inhibited proliferation of lung epithelium, which lowers the number of epithelial cells and could contribute to the halted branching formation and few $Sox2^+$ stalks in the *Prmt5* mutant. In agreement with this, significantly increased epithelial apoptosis was observed in the shortened $Sox2^+$ proximal regions of *Shh;Prmt5* lungs. Notably, our discoveries of partial rescued $Sox2^+$ stalks and no rescue of cell differentiation defects in Noggin-treated *Prmt5* lungs are consistent with the proposed requirement for BMP signaling, which is required for P-D cell fate specification of lung endoderm (Weaver et al., 1999) but not for Clara/ciliated cell differentiation (Tadokoro et al., 2016). However, we think that there are several possible, non-exclusive explanations for the partial

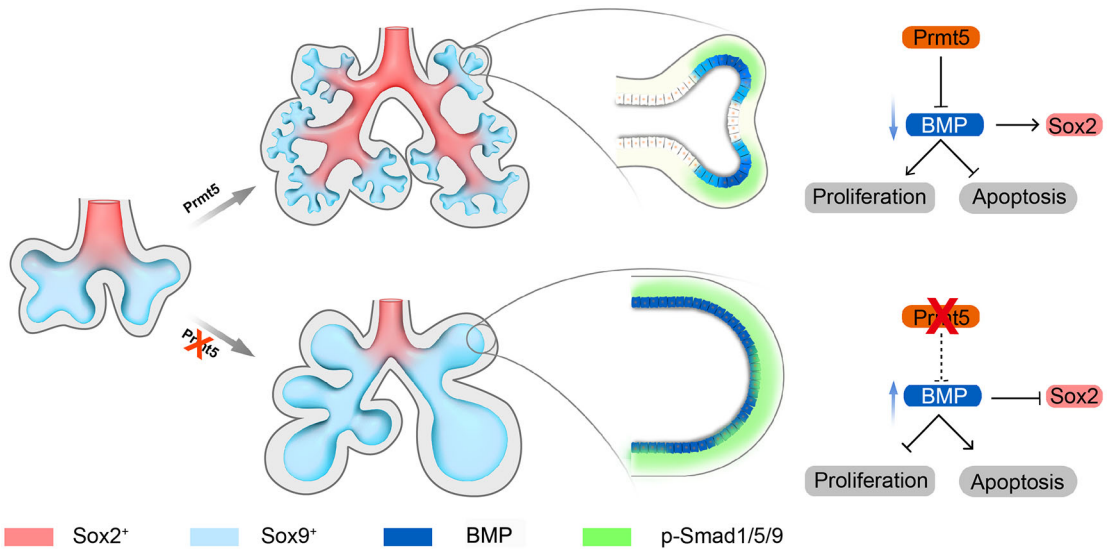

Fig. 8. Working model of Prmt5 regulation of embryonic lung development. During normal lung development, Prmt5 inhibits canonical BMP-Smad1/5/9 signaling, and Bmp4 localization and expression are restricted to the distal tip area, thereby promoting proliferation and limiting apoptosis in the epithelium. In the absence of Prmt5, elevated and unrestricted BMP signaling leads to increased apoptosis and reduced proliferation in lung epithelium, and eventually forms cyst-like lung structures.

rescued Sox2^{+} regions in the *Prmt5* mutant. One is the cell non-autonomous effects of Noggin in the *in vitro* cultured explants (Geng et al., 2011; Lüdtke et al., 2016). Alternatively, other lung-expressed BMP family ligands, Bmp5 and Bmp7 (Bellusci et al., 1996; King et al., 1994), may also contribute to the partial rescue phenotype. Although the transcriptional levels of *Bmp5* and *Bmp7* were not changed in *Shh;Prmt5* mice, we cannot exclude the possibility that signaling by these BMP ligands is blocked by Noggin treatment. Additionally, genes related to cell junction/adhesion and some transcription factors in regulation of lung development were consistently altered in *Prmt5* mutant lungs, as demonstrated by microarray and RNA-seq data, suggesting that these factors were also involved. Further studies are needed to address and evaluate these possibilities.

Many organs of higher organisms are heavily branched structures that arise by an apparently similar process of branching morphogenesis, which is intricately regulated by a conserved network of signaling factors (Affolter et al., 2009). Fgf10 signaling is reported to direct the outgrowth of epithelium in lung (Bellusci et al., 1997b), prostate (Donjacour et al., 2003; Wilhelm and Koopman, 2006), salivary gland (Makarenkova et al., 2009) and pancreas (Bhushan et al., 2001; Pulkkinen et al., 2003), whereas Shh signaling is upregulated by Fgf10 in the lung (Abler et al., 2009; Herriges et al., 2015) and prostate (Pu et al., 2004) during branching. Bmp4 signaling inhibits branching morphogenesis in lung (Bellusci et al., 1996; Wang et al., 2013b), kidney (Chi et al., 2011), prostate (Keil et al., 2015; Lamm et al., 2001) and pancreas (Ahnfelt-Rønne et al., 2010). Whether the Prmt5-BMP-Smad1/5/9 regulatory mechanism identified in this study is conserved during branching morphogenesis in other organs and species needs to be addressed in studies on tissue-specific *Prmt5* knockout mice.

MATERIALS AND METHODS

Animals

The *Prmt5* knockout first mouse line, Prmt5$^{tm2a(EUCOMM)Wtsi}$, was obtained from the European Conditional Mouse Mutagenesis Program (EUCOMM; http://www.knockoutmouse.org). *Prmt5$^{fl/fl}$* allele was generated as previously described (Wang et al., 2015a,b). The lung epithelium-specific *Prmt5* knockout mice (*Shh;Prmt5*) were generated by crossing *Prmt5$^{fl/fl}$* mice with *Shh$^{cre/+}$* mice (Harfe et al., 2004; Harris et al., 2006), which were kindly gifted by Prof. Lin Xinhua (Fudan University). The inducible lung epithelial-specific *Prmt5* knockout mice (*SPC;Prmt5*) were generated by crossing *Prmt5$^{fl/fl}$* mice with *SPC-rtTA* mice (Tichelaar et al., 2000) and *TetO-Cre* mice (Sauer, 1998). Administration of doxycycline started from different gestation stages to the endpoint of the experiment by feeding the pregnant mice with 625 mg/kg of doxycycline-containing food. *Rosa-mTmG* reporter mice and *p21* knockout mice were kindly gifted by Prof. John Speakman [Institute of Genetics and Developmental Biology-Chinese Academy of Sciences (IGDB-CAS)] and Prof. Yuan Weiping (Chinese Academy of Medical Sciences), respectively. The embryos used in these experiments were harvested from time-mated females; noon of the day on which a vaginal plug was detected was considered E0.5. All mice used in this study were bred in the C57BL/6 strain background, and genotyped by genomic DNA PCR using primers listed in Table S3. Mice were housed in a specific pathogen-free condition with a 12 h light/12 h dark cycle in a temperature- and humidity-controlled environment. All animal work was performed in accordance with the guidelines set by the animal welfare committees of the IGDB-CAS.

Lung explant culture

Lungs from control and *Prmt5* mutant embryos were harvested at either E11.5 or E12.5 as indicated. Lungs were placed on a Nuclepore track-etched membrane (Whatman, 110614) and cultured at the air/liquid interface with DMEM-F12 (Invitrogen, C11330500BT) and 10% fetal bovine serum (FBS, Invitrogen, 16000-044). Noggin (Excell, CB055; 500 ng/ml) was added to inhibit BMP signaling in the Noggin rescue experiment. Lungs were cultured in an incubator at 37°C and 5% CO_2 for the indicated time before harvest and analysis. All lung explant culture experiments were repeated three to five times with embryos from at least three pregnant mothers.

Sectional immunofluorescence staining, imaging and quantification

Immunofluorescence staining was performed following a previously published protocol (Liu et al., 2017). Briefly, 8-µm-thick frozen sections were pretreated with 0.5% Triton X-100 in PBS for 15 min at room temperature. After blocking, sections were incubated with primary antibodies overnight at 4°C followed by 2 h of incubation with appropriate secondary antibodies and counterstained with DAPI. The antibodies used are listed in Table S4. Images were acquired using a Leica TCS SP8 confocal microscope and a Nikon Ti-E&N-STORM super resolution microscope system. For quantification, images were obtained from a minimum of five mice per genotype. Cells were counted in at least three different areas of each image for each mouse. Three-dimensional reconstitution images were obtained using Imaris software (Bitplane) and assembled using reconstruction software (Fiala, 2005) from z-stacks of sections.

The p-Smad1/5/9 staining was performed with the Tyramide Signal Amplification (TSA) system (Perkin Elmer LAS, NEL702001KT) following a previously described protocol (Mou et al., 2016). Briefly, 8-µm-thick frozen sections were pretreated with 0.5% Triton X-100 in PBS for 15 min, and endogenous peroxidases were blocked by incubating with 3% H_2O_2 for 30 min. The slides were incubated with p-Smad1/5/9 antibody at 4°C overnight. The next day, the slides were incubated with biotin-conjugated donkey anti-rabbit IgG in 5% BSA/0.2% PBS-Triton X-100 for 2 h. After washing with 0.2% PBS-Triton X-100, the slides were incubated with ABC Elite reagent (Vector, PK-6100) for 2 h and then incubated with TSA working solution for 15 min.

Whole-mount immunofluorescence staining and imaging

Whole-mount staining was performed following a previously published protocol (Metzger et al., 2008; Tang et al., 2011). Briefly, lungs isolated from indicated developmental stages were fixed in 4% paraformaldehyde for 1 h at 4°C and then dehydrated with methanol. Lungs were incubated with E-cadherin or Sox2/Sox9 antibodies (Table S4) overnight at 4°C, followed by 2 h of incubation with appropriate secondary antibodies. Then, the stained lungs were visualized by a Leica MZ16F stereomicroscope.

Histologic analysis, immunohistochemical staining and H&E staining

For histologic analysis, lungs isolated from indicated developmental stages were fixed in 4% (wt/vol) paraformaldehyde (Sigma-Aldrich, P6148) overnight at 4°C and then processed to paraffin (Thermo, 8330) embedding and sectioned at 5 µm. For immunohistochemical staining, sections were deparaffinized and rehydrated. Antigen retrieval was performed using the microwave method. After blocking, sections were incubated with diluted primary antibodies (Table S4) in 0.2% PBS-Triton X-100 overnight at 4°C followed by 1 h of incubation with selected secondary antibodies and counterstained with hematoxylin. H&E staining was performed as described previously (Ying et al., 2015).

RNA extraction and real-time PCR

RNA was prepared using TRIzol reagent (Ambion, 15596) and reverse transcribed with a FastQuant RT Kit (TIANGEN, KR106) according to the manufacturer's protocol. PCR was quantified using SYBR Green in an Agilent Technologies StrataGene Mx3000P system. At least three biological replicates were performed per genotype and three technical replicates were performed for every independent experiment. The mRNA levels were normalized to internal β-actin expression. The primers used are listed in Table S3.

For qRT-PCR on purified mGFP^{+} cells, *Prmt5$^{fl/fl}$;Shh$^{cre/+}$;mTmG* embryonic lungs were homogenized, and mGFP^{+} and mTomato^{+} cell populations were sorted by flow cytometry (BD FACS Aria II).

RNA *in situ* hybridization and TUNEL assay

In situ hybridization on 15-µm frozen sections was performed essentially as described previously (Wang et al., 2013a; Zhang et al., 2014). For each marker, at least three independent specimens were analyzed. TUNEL assay was assessed on 8-µm-thick frozen sections by using an *In Situ* Cell Death Detection Kit (Roche, 11684795910), according to the manufacturer's instructions.

Microarray and RNA-sequencing assays

For microarray analysis, RNA was isolated from E14.5 lungs of three control and three *SPC;Prmt5* embryos. Microarray analysis was performed according to the protocol described previously (Zheng et al., 2013).

For RNA sequencing, total RNA was extracted from E14.5 control and *Shh;Prmt5* lungs. For each sample, seven lungs were collected and pooled. Sequencing libraries were generated using a NEBNext® Ultra™ RNA Library Prep Kit and sequenced on an Illumina HiSeq platform. The 125 bp/150 bp paired-end reads were generated and reads were aligned to the mouse reference genome (mm10) using TopHat v. 2.0.12. HTSeq v. 0.6.1 was used to count the read numbers, and then the fragments per kilobase million (FPKM) value of each gene was calculated based on the length of the gene and read count mapped to this gene. Differential expression analysis was performed using the DESeq R package (1.18.0). The full-sequence dataset was deposited in the GEO database (accession no. GSE108934).

ChIP assays and western blotting

Approximately 20 lungs from E12.5 wild-type mice were isolated and pooled in a ChIP assay as described previously (Ying et al., 2015). Primers for quantitative PCR detection of *Bmp4* chromatin regions are listed in Table S3. Western blotting was performed as described previously (Ying et al., 2015).

Statistical analysis

All experiments were repeated at least three times, and all data are presented as means±s.e.m. Statistical calculations were analyzed by GraphPad Prism version 6 (GraphPad Software, San Diego, CA). A two-tailed unpaired Student's *t*-test was used for the comparison between two experimental groups. For experiments with more than two groups, one-way ANOVA was performed with appropriate multiple comparisons as described in the figure legends. All statistics are representative of biological replicates. $*P<0.05$, $**P<0.01$, n.s., not significant.

Acknowledgements

We thank Shuangbo Kong and Haibin Wang for their input in the *in situ* hybridization experiment.

Competing interests

The authors declare no competing or financial interests.

Author contributions

Conceptualization: Q.L., S.B.; Methodology: Q.L., J.J., H.L., H.W.; Software: J.J., C.Z., J.C.; Validation: Q.L.; Investigation: Q.L., J.J.; Resources: H.W., S.B.; Writing - original draft: Q.L.; Writing - review & editing: Q.L., J.J., H.W., S.B.; Supervision: S.B.; Funding acquisition: Q.L., S.B.

Funding

This work was supported by The National Natural Science Foundation of China (grant numbers 31601164, 31571379, 31730051 and 31371378).

Supplementary information

Supplementary information available online at
http://jcs.biologists.org/lookup/doi/10.1242/jcs.217406.supplemental

References

Abler, L. L., Mansour, S. L. and Sun, X. (2009). Conditional gene inactivation reveals roles for Fgf10 and Fgfr2 in establishing a normal pattern of epithelial branching in the mouse lung. *Dev. Dyn.* **238**, 1999-2013.

Affolter, M., Zeller, R. and Caussinus, E. (2009). Tissue remodelling through branching morphogenesis. *Nat. Rev. Mol. Cell Biol.* **10**, 831-842.

Ahnfelt-Rønne, J., Ravassard, P., Pardanaud-Glavieux, C., Scharfmann, R. and Serup, P. (2010). Mesenchymal bone morphogenetic protein signaling is required for normal pancreas development. *Diabetes* **59**, 1948-1956.

Alanis, D. M., Chang, D. R., Akiyama, H., Krasnow, M. A. and Chen, J. (2014). Two nested developmental waves demarcate a compartment boundary in the mouse lung. *Nat. Commun.* **5**, 3923.

Ancelin, K., Lange, U. C., Hajkova, P., Schneider, R., Bannister, A. J., Kouzarides, T. and Surani, M. A. (2006). Blimp1 associates with Prmt5 and directs histone arginine methylation in mouse germ cells. *Nat. Cell Biol.* **8**, 623-630.

Bellusci, S., Henderson, R., Winnier, G., Oikawa, T. and Hogan, B. L. (1996). Evidence from normal expression and targeted misexpression that bone morphogenetic protein (Bmp-4) plays a role in mouse embryonic lung morphogenesis. *Development* **122**, 1693-1702.

Bellusci, S., Furuta, Y., Rush, M. G., Henderson, R., Winnier, G. and Hogan, B. L. (1997a). Involvement of Sonic hedgehog (Shh) in mouse embryonic lung growth and morphogenesis. *Development* **124**, 53-63.

Bellusci, S., Grindley, J., Emoto, H., Itoh, N. and Hogan, B. L. (1997b). Fibroblast growth factor 10 (FGF10) and branching morphogenesis in the embryonic mouse lung. *Development* **124**, 4867-4878.

Bezzi, M., Teo, S. X., Muller, J., Mok, W. C., Sahu, S. K., Vardy, L. A., Bonday, Z. Q. and Guccione, E. (2013). Regulation of constitutive and alternative splicing by PRMT5 reveals a role for Mdm4 pre-mRNA in sensing defects in the spliceosomal machinery. *Genes Dev.* **27**, 1903-1916.

Bhushan, A., Itoh, N., Kato, S., Thiery, J. P., Czernichow, P., Bellusci, S. and Scharfmann, R. (2001). Fgf10 is essential for maintaining the proliferative capacity of epithelial progenitor cells during early pancreatic organogenesis. *Development* **128**, 5109-5117.

Biggar, K. K. and Li, S. S.-C. (2015). Non-histone protein methylation as a regulator of cellular signalling and function. *Nat. Rev. Mol. Cell Biol.* **16**, 5-17.

Chi, L., Saarela, U., Railo, A., Prunskaite-Hyyryläinen, R., Skovorodkin, I., Anthony, S., Katsu, K., Liu, Y., Shan, J., Salgueiro, A. M. et al. (2011). A secreted BMP antagonist, Cer1, fine tunes the spatial organization of the ureteric bud tree during mouse kidney development. *PLoS ONE* **6**, e27676.

Di Lorenzo, A. and Bedford, M. T. (2011). Histone arginine methylation. *FEBS Lett.* **585**, 2024-2031.

Domyan, E. T. and Sun, X. (2011). Patterning and plasticity in development of the respiratory lineage. *Dev. Dyn.* **240**, 477-485.

Domyan, E. T., Ferretti, E., Throckmorton, K., Mishina, Y., Nicolis, S. K. and Sun, X. (2011). Signaling through BMP receptors promotes respiratory identity in the foregut via repression of Sox2. *Development* **138**, 971-981.

Donjacour, A. A., Thomson, A. A. and Cunha, G. R. (2003). FGF-10 plays an essential role in the growth of the fetal prostate. *Dev. Biol.* **261**, 39-54.

Fiala, J. C. (2005). Reconstruct: a free editor for serial section microscopy. *J. Microsc.* **218**, 52-61.

Geng, Y., Dong, Y., Yu, M., Zhang, L., Yan, X., Sun, J., Qiao, L., Geng, H., Nakajima, M., Furuichi, T. et al. (2011). Follistatin-like 1 (Fstl1) is a bone morphogenetic protein (BMP) 4 signaling antagonist in controlling mouse lung development. *Proc. Natl. Acad. Sci. USA* **108**, 7058-7063.

Gontan, C., de Munck, A., Vermeij, M., Grosveld, F., Tibboel, D. and Rottier, R. (2008). Sox2 is important for two crucial processes in lung development: branching morphogenesis and epithelial cell differentiation. *Dev. Biol.* **317**, 296-309.

Harfe, B. D., Scherz, P. J., Nissim, S., Tian, H., McMahon, A. P. and Tabin, C. J. (2004). Evidence for an expansion-based temporal Shh gradient in specifying vertebrate digit identities. *Cell* **118**, 517-528.

Harris, K. S., Zhang, Z., McManus, M. T., Harfe, B. D. and Sun, X. (2006). Dicer function is essential for lung epithelium morphogenesis. *Proc. Natl. Acad. Sci. USA* **103**, 2208-2213.

Herriges, M. and Morrisey, E. E. (2014). Lung development: orchestrating the generation and regeneration of a complex organ. *Development* **141**, 502-513.

Herriges, J. C., Yi, L., Hines, E. A., Harvey, J. F., Xu, G., Gray, P. A., Ma, Q. and Sun, X. (2012). Genome-scale study of transcription factor expression in the branching mouse lung. *Dev. Dyn.* **241**, 1432-1453.

Herriges, J. C., Verheyden, J. M., Zhang, Z., Sui, P., Zhang, Y., Anderson, M. J., Swing, D. A., Zhang, Y., Lewandoski, M. and Sun, X. (2015). FGF-regulated ETV transcription factors control FGF-SHH feedback loop in lung branching. *Dev. Cell* **35**, 322-332.

Hogan, B. L. (1996). Bone morphogenetic proteins: multifunctional regulators of vertebrate development. *Genes Dev.* **10**, 1580-1594.

Holleville, N., Quilhac, A., Bontoux, M. and Monsoro-Burq, A.-H. (2003). BMP signals regulate Dlx5 during early avian skull development. *Dev. Biol.* **257**, 177-189.

Hollnagel, A., Oehlmann, V., Heymer, J., Rüther, U. and Nordheim, A. (1999). Id genes are direct targets of bone morphogenetic protein induction in embryonic stem cells. *J. Biol. Chem.* **274**, 19838-19845.

Hu, D., Gur, M., Zhou, Z., Gamper, A., Hung, M.-C., Fujita, N., Lan, L., Bahar, I. and Wan, Y. (2015). Interplay between arginine methylation and ubiquitylation regulates KLF4-mediated genome stability and carcinogenesis. *Nat. Commun.* **6**, 8419.

Hyatt, B. A., Shangguan, X. and Shannon, J. M. (2002). BMP4 modulates fibroblast growth factor-mediated induction of proximal and distal lung differentiation in mouse embryonic tracheal epithelium in mesenchyme-free culture. *Dev. Dyn.* **225**, 153-165.

Jen, Y., Manova, K. and Benezra, R. (1996). Expression patterns of Id1, Id2, and Id3 are highly related but distinct from that of Id4 during mouse embryogenesis. *Dev. Dyn.* **207**, 235-252.
Keil, K. P., Altmann, H. M., Abler, L. L., Hernandez, L. L. and Vezina, C. M. (2015). Histone acetylation regulates prostate ductal morphogenesis through a bone morphogenetic protein-dependent mechanism. *Dev. Dyn.* **244**, 1404-1414.
King, J. A., Marker, P. C., Seung, K. J. and Kingsley, D. M. (1994). BMP5 and the molecular, skeletal, and soft-tissue alterations in short ear mice. *Dev. Biol.* **166**, 112-122.
Lamm, M. L. G., Podlasek, C. A., Barnett, D. H., Lee, J., Clemens, J. Q., Hebner, C. M. and Bushman, W. (2001). Mesenchymal factor bone morphogenetic protein 4 restricts ductal budding and branching morphogenesis in the developing prostate. *Dev. Biol.* **232**, 301-314.
Lebeche, D., Malpel, S. and Cardoso, W. V. (1999). Fibroblast growth factor interactions in the developing lung. *Mech. Dev.* **86**, 125-136.
Lee, J. and Bedford, M. T. (2002). PABP1 identified as an arginine methyltransferase substrate using high-density protein arrays. *EMBO Rep.* **3**, 268-273.
Li, Q., Zhao, Y., Yue, M., Xue, Y. and Bao, S. (2016). The Protein Arginine Methylase 5 (PRMT5/SKB1) gene is required for the maintenance of root stem cells in response to DNA damage. *J. Genet. Genom.* **43**, 187-197.
Liu, Y. and Hogan, B. L. M. (2002). Differential gene expression in the distal tip endoderm of the embryonic mouse lung. *Gene Expr. Patterns* **2**, 229-233.
Liu, C., Mei, M., Li, Q., Roboti, P., Pang, Q., Ying, Z., Gao, F., Lowe, M. and Bao, S. (2017). Loss of the golgin GM130 causes Golgi disruption, Purkinje neuron loss, and ataxia in mice. *Proc. Natl Acad. Sci. USA* **114**, 346-351.
Lüdtke, T. H., Rudat, C., Wojahn, I., Weiss, A.-C., Kleppa, M.-J., Kurz, J., Farin, H. F., Moon, A., Christoffels, V. M. and Kispert, A. (2016). Tbx2 and Tbx3 act downstream of Shh to maintain canonical Wnt signaling during branching morphogenesis of the murine lung. *Dev. Cell* **39**, 239-253.
Makarenkova, H. P., Hoffman, M. P., Beenken, A., Eliseenkova, A. V., Meech, R., Tsau, C., Patel, V. N., Lang, R. A. and Mohammadi, M. (2009). Differential interactions of FGFs with heparan sulfate control gradient formation and branching morphogenesis. *Sci. Signal.* **2**, ra55.
Metzger, R. J., Klein, O. D., Martin, G. R. and Krasnow, M. A. (2008). The branching programme of mouse lung development. *Nature* **453**, 745-750.
Michos, O., Panman, L., Vintersten, K., Beier, K., Zeller, R. and Zuniga, A. (2004). Gremlin-mediated BMP antagonism induces the epithelial-mesenchymal feedback signaling controlling metanephric kidney and limb organogenesis. *Development* **131**, 3401-3410.
Min, H., Danilenko, D. M., Scully, S. A., Bolon, B., Ring, B. D., Tarpley, J. E., DeRose, M. and Simonet, W. S. (1998). Fgf-10 is required for both limb and lung development and exhibits striking functional similarity to Drosophila branchless. *Genes Dev.* **12**, 3156-3161.
Minoo, P., Su, G., Drum, H., Bringas, P. and Kimura, S. (1999). Defects in tracheoesophageal and lung morphogenesis in Nkx2.1(−/−) mouse embryos. *Dev. Biol.* **209**, 60-71.
Morrisey, E. E. and Hogan, B. L. M. (2010). Preparing for the first breath: genetic and cellular mechanisms in lung development. *Dev. Cell* **18**, 8-23.
Mou, H., Vinarsky, V., Tata, P. R., Brazauskas, K., Choi, S. H., Crooke, A. K., Zhang, B., Solomon, G. M., Turner, B., Bihler, H. et al. (2016). Dual SMAD signaling inhibition enables long-term expansion of diverse epithelial basal cells. *Cell Stem Cell* **19**, 217-231.
Moustakas, A. and Heldin, C.-H. (2009). The regulation of TGFbeta signal transduction. *Development* **136**, 3699-3714.
Norrie, J. L., Li, Q., Co, S., Huang, B.-L., Ding, D., Uy, J. C., Ji, Z., Mackem, S., Bedford, M. T., Galli, A. et al. (2016). PRMT5 is essential for the maintenance of chondrogenic progenitor cells in the limb bud. **143**, 4608-4619.
Pepicelli, C. V., Lewis, P. M. and McMahon, A. P. (1998). Sonic hedgehog regulates branching morphogenesis in the mammalian lung. *Curr. Biol.* **8**, 1083-1086.
Perl, A.-K. T., Kist, R., Shan, Z., Scherer, G. and Whitsett, J. A. (2005). Normal lung development and function after Sox9 inactivation in the respiratory epithelium. *Genesis* **41**, 23-32.
Pu, Y., Huang, L. and Prins, G. S. (2004). Sonic hedgehog-patched Gli signaling in the developing rat prostate gland: lobe-specific suppression by neonatal estrogens reduces ductal growth and branching. *Dev. Biol.* **273**, 257-275.
Pulkkinen, M.-A., Spencer-Dene, B., Dickson, C. and Otonkoski, T. (2003). The IIIb isoform of fibroblast growth factor receptor 2 is required for proper growth and branching of pancreatic ductal epithelium but not for differentiation of exocrine or endocrine cells. *Mech. Dev.* **120**, 167-175.
Que, J., Okubo, T., Goldenring, J. R., Nam, K.-T., Kurotani, R., Morrisey, E. E., Taranova, O., Pevny, L. H. and Hogan, B. L. M. (2007). Multiple dose-dependent roles for Sox2 in the patterning and differentiation of anterior foregut endoderm. *Development* **134**, 2521-2531.
Rawlins, E. L. (2008). Lung epithelial progenitor cells: lessons from development. *Proc. Am. Thorac. Soc.* **5**, 675-681.
Rock, J. R. and Hogan, B. L. M. (2011). Epithelial Progenitor Cells in Lung Development, Maintenance, Repair, and Disease. *Annu. Rev. Cell Dev. Biol.* **27**, 493-512.
Sauer, B. (1998). Inducible gene targeting in mice using the Cre/lox system. *Methods* **14**, 381-392.
Sekine, K., Ohuchi, H., Fujiwara, M., Yamasaki, M., Yoshizawa, T., Sato, T., Yagishita, N., Matsui, D., Koga, Y., Itoh, N. et al. (1999). Fgf10 is essential for limb and lung formation. *Nat. Genet.* **21**, 138-141.
Shen, T., Sun, C., Zhang, Z., Xu, N., Duan, X., Feng, X.-H. and Lin, X. (2014). Specific control of BMP signaling and mesenchymal differentiation by cytoplasmic phosphatase PPM1H. *Cell Res.* **24**, 727-741.
Stopa, N., Krebs, J. E. and Shechter, D. (2015). The PRMT5 arginine methyltransferase: many roles in development, cancer and beyond. *Cell. Mol. Life Sci.* **72**, 2041-2059.
Tadokoro, T., Gao, X., Hong, C. C., Hotten, D. and Hogan, B. L. M. (2016). BMP signaling and cellular dynamics during regeneration of airway epithelium from basal progenitors. *Development* **143**, 764-773.
Tae, S., Karkhanis, V., Velasco, K., Yaneva, M., Erdjument-Bromage, H., Tempst, P. and Sif, S. (2011). Bromodomain protein 7 interacts with PRMT5 and PRC2, and is involved in transcriptional repression of their target genes. *Nucleic Acids Res.* **39**, 5424-5438.
Tang, N., Marshall, W. F., McMahon, M., Metzger, R. J. and Martin, G. R. (2011). Control of mitotic spindle angle by the RAS-regulated ERK1/2 pathway determines lung tube shape. *Science* **333**, 342-345.
Tee, W.-W., Pardo, M., Theunissen, T. W., Yu, L., Choudhary, J. S., Hajkova, P. and Surani, M. A. (2010). Prmt5 is essential for early mouse development and acts in the cytoplasm to maintain ES cell pluripotency. *Genes Dev.* **24**, 2772-2777.
Tichelaar, J. W., Lu, W. and Whitsett, J. A. (2000). Conditional expression of fibroblast growth factor-7 in the developing and mature lung. *J. Biol. Chem.* **275**, 11858-11864.
Wang, X., Zhang, Y., Ma, Q., Zhang, Z., Xue, Y., Bao, S. and Chong, K. (2007). SKB1-mediated symmetric dimethylation of histone H4R3 controls flowering time in Arabidopsis. *EMBO J.* **26**, 1934-1941.
Wang, Q., Lu, J., Zhang, S., Wang, S., Wang, W., Wang, B., Wang, F., Chen, Q., Duan, E., Leitges, M. et al. (2013a). Wnt6 is essential for stromal cell proliferation during decidualization in mice. *Biol. Reprod.* **88**, 5.
Wang, Y., Tian, Y., Morley, M. P., Lu, M. M., Demayo, F. J., Olson, E. N. and Morrisey, E. E. (2013b). Development and regeneration of Sox2+ endoderm progenitors are regulated by a Hdac1/2-Bmp4/Rb1 regulatory pathway. *Dev. Cell* **24**, 345-358.
Wang, Y., Li, Q., Liu, C., Han, F., Chen, M., Zhang, L., Cui, X., Qin, Y., Bao, S. and Gao, F. (2015a). Protein arginine methyltransferase 5 (Prmt5) is required for germ cell survival during mouse embryonic development. *Biol. Reprod.* **92**, 104.
Wang, Y., Zhu, T., Li, Q., Liu, C., Han, F., Chen, M., Zhang, L., Cui, X., Qin, Y., Bao, S. et al. (2015b). Prmt5 is required for germ cell survival during spermatogenesis in mice. *Sci. Rep.* **5**, 11031.
Weaver, M., Yingling, J. M., Dunn, N. R., Bellusci, S. and Hogan, B. L. (1999). Bmp signaling regulates proximal-distal differentiation of endoderm in mouse lung development. *Development* **126**, 4005-4015.
Weaver, M., Dunn, N. R. and Hogan, B. L. (2000). Bmp4 and Fgf10 play opposing roles during lung bud morphogenesis. *Development* **127**, 2695-2704.
Wells, J. M. and Melton, D. A. (1999). Vertebrate endoderm development. *Annu. Rev. Cell Dev. Biol.* **15**, 393-410.
Wilhelm, D. and Koopman, P. (2006). The makings of maleness: towards an integrated view of male sexual development. *Nat. Rev. Genet.* **7**, 620-631.
Xu, X., Hoang, S., Mayo, M. W. and Bekiranov, S. (2010). Application of machine learning methods to histone methylation ChIP-Seq data reveals H4R3me2 globally represses gene expression. *BMC Bioinformatics* **11**, 396.
Ying, Z., Mei, M., Zhang, P., Liu, C., He, H., Gao, F. and Bao, S. (2015). Histone arginine methylation by PRMT7 controls germinal center formation via regulating Bcl6 transcription. *J. Immunol.* **195**, 1538-1547.
Yue, M., Li, Q., Zhang, Y., Zhao, Y., Zhang, Z. and Bao, S. (2013). Histone H4R3 methylation catalyzed by SKB1/PRMT5 is required for maintaining shoot apical meristem. *PLoS ONE* **8**, e83258.
Zhang, Z., Zhang, S., Zhang, Y., Wang, X., Li, D., Li, Q., Yue, M., Li, Q., Zhang, Y.-E., Xu, Y. et al. (2011). Arabidopsis floral initiator SKB1 confers high salt tolerance by regulating transcription and pre-mRNA splicing through altering histone H4R3 and small nuclear ribonucleoprotein LSM4 methylation. *Plant Cell* **23**, 396-411.
Zhang, S., Kong, S., Wang, B., Cheng, X., Chen, Y., Wu, W., Wang, Q., Shi, J., Zhang, Y., Wang, S. et al. (2014). Uterine Rbpj is required for embryonic-uterine orientation and decidual remodeling via Notch pathway-independent and -dependent mechanisms. *Cell Res.* **24**, 925-942.
Zhang, T., Günther, S., Looso, M., Künne, C., Krüger, M., Kim, J., Zhou, Y. and Braun, T. (2015). Prmt5 is a regulator of muscle stem cell expansion in adult mice. *Nat. Commun.* **6**, 7140.
Zheng, C., Miao, X., Li, Y., Huang, Y., Ruan, J., Ma, X., Wang, L., Wu, C.-I. and Cai, J. (2013). Determination of genomic copy number alteration emphasizing a restriction site-based strategy of genome re-sequencing. *Bioinformatics* **29**, 2813-2821.
Zhou, Z., Sun, X., Zou, Z., Sun, L., Zhang, T., Guo, S., Wen, Y., Liu, L., Wang, Y., Qin, J. et al. (2010). PRMT5 regulates Golgi apparatus structure through methylation of the golgin GM130. *Cell Res.* **20**, 1023-1033.